Arif, M. and Jones, F. and Barifcani, A. and Iglauer, S. 2017. Influence of surface chemistry on interfacial properties of low to high rank coal seams. Fuel. 194: pp. 211-221.

Influence of surface chemistry on interfacial properties of low to high rank coal seams

Muhammad Arif[1*], Franca Jones[2], Ahmed Barifcani[1], Stefan Iglauer[1]

[1]Curtin University, Department of Petroleum Engineering, 26 Dick Perry Avenue, 6151 Kensington, Western Australia; phone: +61 8 9266 7703

[2]Department of Applied Chemistry, Kent Street, Curtin University, Bentley, WA, 6102

[*]Corresponding author

Phone: +61 8 9266 7703

Fax: +61 8 9266 7063

Email: muhammad.arif@curtin.edu.au

Abstract

Wettability of CO_2/water/coal systems is a fundamental petro-physical parameter, which governs the fluid flow and distribution in coal seams and thus directly affects CO_2-storage and methane recovery from unmineable coal seams. The recognition of wettability of coal/CO_2/brine systems help to de-risk CO_2-storage and enhanced methane recovery projects in coal seams. To understand the factors influencing the wetting characteristics of coals, a detailed examination and characterization of coal surface chemistry is essential and literature data in this context is missing. We thus measured zeta potentials as a function of temperature (298 K-343 K), brine salinity (0 wt% NaCl – 5 wt% NaCl) and salt type (NaCl, $CaCl_2$ and $MgCl_2$) for coals of low, medium and high ranks. Further, we measured water advancing and receding contact angles as a function of temperature and salinity for the same experimental matrix in order to associate wettability changes to the surface charge at the coal/brine interface.

Moreover, coal surfaces were investigated by Fourier transformed infrared (FTIR) spectroscopy and the surface functional groups responsible for a particular wetting behaviour

were identified. We found that zeta potential increased with temperature, salinity and cation valency. Both advancing and receding contact angles decreased with temperature, and increased with salinity and cation valency irrespective of the coal rank. Finally the XRD measurements and infrared spectra revealed that the presence of polar surface functional groups (e.g. Si-OH and carboxylic acid groups) which is responsible for the hydrophilic behaviour of low rank coals and the absence of these groups in high rank coal is responsible for their hydrophobic behaviour even at lower pressure. The high rank coal seams at high pressure are better for CO_2 storage and methane recovery.

1. Introduction

The injection of CO_2 in depleted oil and gas reservoirs or deep saline aquifers is capable of trapping tremendous amounts of CO_2 and thus reduce anthropogenic CO_2 emissions [1-3]. Certain trapping mechanisms render CO_2 immobile in the porous medium, and these are structural trapping [4-7], residual or capillary trapping [8,9], dissolution or solubility trapping [10] and mineral trapping [11]. Coal seams, too, offer enormous potential for CO_2 storage and enhanced methane recovery by means of preferential adsorption of CO_2 [12,13]. Adsorption is the major CO_2 trapping mechanism in unminable coal seams and the wettability of the specific CO_2/brine/coal system plays a significant role in this context [12,14]. Typically, the adsorption capacity of CO_2 is higher than that of methane, consequently, CO_2 displaces methane toward the production well and itself gets sorbed within the micropores of the coal seam and remains trapped [12]. Moreover, Arif et al. [12] pointed out that higher CO_2-wettability would lead to higher CO_2-adsorption and thus higher storage [12].

Although coal wettability has been characterized as a function of pressure, temperature, salinity and coal rank [12,15], the factors responsible for a particular wetting behaviour are so far unclear. Specifically, the knowledge and characterization of coal surface chemistry is essential to understand the factors that influence its wettability [16,17]. In this context, zeta potential is used to probe the double layer at the surface of the coal. The nature of the double layer affects the repulsion/attraction of system's components, and depends upon the physicochemical properties of all components in the overall system [18]. Thus, what occurs at the brine/mineral or brine/rock interface (at a particular temperature and brine salinity) is strongly affected by the electrical double layer and studies have shown that this double layer is closely related to wettability [19-21].

We thus examined the electrochemical behaviour of coal by measuring zeta potentials as a function of temperature (298 K-343 K), salinity (0 wt% NaCl-5 wt% NaCl), salt type (NaCl, $CaCl_2$ and $MgCl_2$) and coal rank (low, medium and high rank) to allow surface characterization for broad range of conditions. In addition, following the same experimental matrix, we measured advancing and receding contact angles for air/coal/brine systems (at ambient pressure). The associated trends were analysed systematically and relationships were developed between zeta potential and wettability. We found that the zeta potential increased with increasing rank and increasing salinity and contact angles also increased with increasing rank and salinity, implying a positive correlation between zeta potential and wettability. However, with increasing temperature zeta potential increased but contact angle decreased, implying that correlation with respect to temperature is inconsistent. Moreover, the zeta potential results were also compared to our published contact angle data at high pressure, and we hypothesized that zeta potential at high pressure may follow similar trends as those at ambient pressure.

Further, in order to evaluate the impact of coal rank on wettability of the coal/CO_2/brine systems, we conducted Fourier transformed infrared spectroscopy (FTIR) measurements on the three coal samples (low, medium and high rank) and thoroughly characterized the surface functional groups. The results demonstrated that the abundance of OH and carboxylic acid groups on the low rank coal is responsible for the hydrophilic nature of lignite and the lack of these groups explains the hydrophobic nature of high rank coal (semi-anthracite).

2. Experimental Methodology

2.1. Fluid/sample preparation

Three coal samples [high rank (semi anthracite; from Hazelton, Pennsylvania, USA), medium rank (medium volatile bituminous; from Morgantown, West Virginia, USA), and low rank (lignite; from North Dakota, USA; Table 1)] were used in this research. The samples were cut to cuboid shape (~1cm x 1cm x 0.5cm) or crushed into fine powder (particle size ~30 microns) using milling equipment (Labtechnics Adelaide, Model TP-4/5, and Oscillation: 50Hz). The powdered samples were then placed in an oven at 90°C for 12 hours until the weight became constant.

Coal/brine composite samples for all coal ranks were prepared by adding 2wt% coal powder to aqueous salt solutions composed of DI water (0M), 1wt% NaCl (0.17M), 5wt% NaCl (0.855M), 1wt% $CaCl_2$ (0.27M), and 1wt% $MgCl_2$ (0.305M). Note: the numbers in brackets represent the equivalent ionic strength of electrolyte which is typically preferred while comparing different types of salt of same strength. In this paper, we mainly used wt% to express salinity, however, for salts comparison we used ionic strength (Section 3.3). Moreover, the alternative common units to express salinity are 'mg/L' and 'ppm'.

Materials used were de-ionized water (Conductivity: 0.02 mS/cm) and brine comprising of NaCl, $CaCl_2$ and $MgCl_2$ (Salts Source: Scharlab s.l., Spain, Purity: $\geq$ 0.995 mass%). The solutions were covered with parafilm and stirred for 5 hours using a magnetic stirrer at 40 °C to ensure homogenous dispersion of the solid powder within the base liquid. The dispersions were then used for the zeta potential measurements. For contact angle measurements, the cuboid samples (low, medium and high rank coal) were selected and for spectroscopic measurements samples were used in powdered form.

2.2. Zeta potential measurements

Zeta potential was measured on a Zetasizer Nano ZS (Malvern instrument). The coal dispersion was placed in a folded capillary cell and sealed at the top. The zeta potential was measured for coal/DI-water for high, medium and low rank coals at 298 K, 308 K, 323 K and 343 K to investigate the effect of temperature on zeta potential. Moreover, the effect of salinity and cation type was analysed for coal dispersed in 1 wt% NaCl, 5 wt% NaCl, 1 wt% $CaCl_2$ and 1 wt% $MgCl_2$ brine. The measurements were repeated three times and the standard deviation of zeta potential measurements was 3 mV at 298 K, ~2.5 mV at 308 K and ~1.5 mV at 323 K and 343 K. Moreover, for higher salinities (5wt% NaCl), standard deviation was also high (3 mV). We used error bars to graphically represent the standard deviation in our results. We observed that the sources of error in zeta potential measurements are evaporation, time lapse between sample preparations to actual measurement, degree of homogeneity of mixing, size of coal particle and electrolyte strength. If these factors are not properly addressed the Zetasizer Nano ZS may give different quality of measurements. We here reported the best three set of measurements which we observed.

123 *2.3. Petrology, Ultimate and Proximate Analysis*

124 The results of the proximate, ultimate and petrological analysis and the internal properties
125 (density and volume) of the coal samples are listed in Table 1. Note that coal samples of
126 different rank differ mainly in volatile matter, moisture, fixed carbon and vitrinite reflectance
127 [22]. Petrology was analysed in accordance with Australian Standard AS2856 and ISO7404;
128 proximate analysis was conducted using standards AS1038.3, ISO11722 and ASTM D3172-
129 07a, and ultimate analysis was performed using standards AS1038.6 and ISO 609.
130

131 **Table 1.** Properties of coal samples used.

Sample	Rank	Semi-Anthracite	Medium-volatile Bituminous	Lignite
	Geological Location	Hazelton, Pennsylvania	Morgantown, West Virginia	North Dakota
	Overall rank (used in this work)	High rank	Medium rank	Low rank
Petrology	Vitrinite Reflectance (R_o, %*)	3.92	0.82	0.35
	Vitrinite (%)	89.6	73.1	83
	Liptinite (%)	0	3.4	4
	Inertinite (%)	7.6	18.8	10.8
	Minerals (%)	2.8	4.7	2.1
Proximate analysis	Moisture (air dried, %)	2.6	2	16.3
	Ash (%)	9.7	6.4	7.8
	Volatile Matter (%)	2.9	32.4	34.8
	Fixed carbon (%)	84.9	59.2	41.1
Ultimate analysis	Ash (%)	9.7	6.4	7.8
	Carbon (%)	82.6	78.6	54.6
	Total Hydrogen (%)	2.35	5.07	5.27
	Hydrogen (%)	2.06	4.85	3.45
	Nitrogen (%)	1.16	1.54	0.62
	Total Sulphur (%)	0.8	0.99	0.66
	Oxygen by difference (%)	3.68	7.62	2.87
Properties	Bulk density (g/cc)	1.30	1.28	1.44
	Dry sample volume (cc)	16.55	12.77	4.26
	Dry mass (g)	21.17	16.194	6.159

132 * All percentages in above table represent weight percent.

133

134 *2.4. pH measurements*

135 The pH values of the solutions were measured at 298 K using a pH meter (model: Orion 420+
136 and a Thermofisher pH probe, accuracy: ±0.005 pH), the results of which are tabulated in Table
137 2. These pH measurements are helpful for a) explanation of zeta potential results as a function
138 of coal rank and brine salinity, and b) precise comparison with zeta potential literature data.

139

140 **Table 2.** Measured pH values of the solutions used.

Electrolyte	pH values		
	Anthracite*	Bituminous*	Lignite*
DI-water	7.09	6.78	6.78
1wt% NaCl	8.13	7.37	6.42
5wt% NaCl	7.97	7.05	6.03
1wt% $CaCl_2$	7.57	6.96	5.48
1wt% $MgCl_2$	8.21	8	5.86

141 *All solutions contained 2 wt% coal powder.

142

143 *2.5. Infrared spectroscopy*

144 Fourier Transformed Infrared spectroscopy was performed using a Nicolet iS50-FTIR
145 instrument (from Thermo Scientific) at 4 cm^{-1} resolution. The powdered sample was placed on
146 a diamond attenuated total reflection (ATR) crystal and pressed into contact. A total of 64 scans
147 were added to generate the final infrared spectrum and the internally available ATR correction
148 was applied to each spectrum with the software (which was supplied by the manufacturer with
149 the instrument).

150

151 *2.6. XRD analysis*

152 XRD analysis was carried out on the three coal samples and minerals were detected in each
153 sample (Table 3). It is evident that the coal mainly comprised of quartz and kaolinite, however,
154 overall mineralogy of these coals is different.

Table 3. Mineral identified by XRD in the three coal samples investigated.

Mineral name	Chemical formula	High rank coal (semi-anthracite)	Medium rank coal (medium volatile bituminous)	Low rank coal (lignite)
Illite	$(K,H_3O)Al_2Si_3AlO_{10}(OH)_2$	34	17	_
Quartz	SiO_2	21	41	76
Kaolinite	$Al_2Si_2O_5(OH)_4$	24	30	24
Anatase	TiO_2	21	_	_
Montmorillonite	$HAl_2CaO.5O_{12}Si_4$	_	6	_
Illite-montmorillonite	$KAl_4(Si,Al)_8O_{10}(OH)_4.4H_2O$	_	6	_

2.7. Contact angle measurements

Contact angles were measured using the pendant drop titled plate technique [23], the schematic of the experimental apparatus has been published previously [12]. The coal substrates were placed in the cell and temperature was set to a desired value (298 K, 308 K, 323 K or 343 K within ± 1 K). Coal surfaces were washed with acetone and then cleaned with air plasma for 2 min (within this selected time the error in contact angle measurements was minimum) and this selected time was neither too short to compromise on the surface contaminants (which need to be removed, [24]) and neither too intense to allow the removal of natural particles from the coal surfaces [12]. A few studies, however, report different coal-surface cleaning methods, e.g. the use of wet polish with abrasive papers, which were then removed by ultrasonic cleaning [14,25].

Subsequently brine was pumped with a high precision syringe pump (ISCO Teledyne 500D) resulting in a droplet of de-gassed brine (vacuumed for 12 h) being dispensed onto the substrate (in air, at ambient pressure and the pre-set temperature) by means of a needle. At the leading edge of the droplet, just before the droplet started to move, the angle between coal surface and the brine interface was measured as the advancing contact angle (θ_a) whereas the receding contact angle (θ_r) was measured at the trailing edge of the droplet. A high performance video camera (Basler scA 640–70 fm, pixel size = 7.4 lm; frame rate = 71 fps; Fujinon CCTV lens: HF35HA-1B; 1:1.6/35 mm) recorded the entire process, and contact angles were measured on images extracted from the movie files. The standard deviation of these measurements was ±4°

based on measurements repeated thrice and is shown by error bars in the results. The measurements were done on one sample each of low, medium and high rank. The coal samples may vary in terms of composition, thus the conclusions drawn in the study may vary depending upon the composition of the coal samples under investigation. In fact, our results revealed that difference in coal rank (e.g. low, medium and high rank, which are obviously different in composition) leads to different zeta potential (at the same operating conditions) which leads to different wettability (discussed in detail in section 3.4).

3. Results and discussion

In order to understand the factors influencing wettability of coal seams, we examined the surface properties of coals. The results lead to a broad understanding of the factors responsible for the distinct wetting characteristics of coals as a function of coal rank, pressure, temperature and brine salinity and thus the results help to precisely understand fluid flow and distribution in coal seams. This information can be used to optimize CO_2-storage and (enhanced) methane recovery projects. Below the influence of each individual parameter is discussed in detail.

3.1. Effect of temperature on zeta potential and contact angle

We found a clear and consistent temperature dependence trend of contact angle and zeta potential for coal/DI water systems. Zeta potentials of these systems increased with increasing temperature within the experimental error (at constant ambient pressure, Figure 1), irrespective of coal rank. Moreover, the advancing and receding water contact angles decreased with temperature for all coal ranks (Figure 2, consistent with [12]). The increase in zeta potential with increasing temperature implies a surface with more screening ions within the double layer at higher temperatures which in turn gives a more water-wet coal surface, i.e. the observed behaviour is different than previously reported behaviour [26].

Specifically, for the high rank coal (semi-anthracite), the zeta potential increased from -23.1 mV to 2.63 mV when temperature increased from 298 K to 343 K (Figure 1). For the same temperature increase, θ_a decreased from 59° to 32° and θ_r decreased from 52° to 27° (Figure 2). Similar trends were found for medium and low rank coals i.e. the zeta potentials of coal/DI water increased with temperature (Figure 1) and corresponding θ_a and θ_r decreased with temperature. For instance, for the medium rank coal (medium volatile bituminous), the zeta

potential increased from -24.8 mV to 0.236 mV when temperature increased from 298 K to 343 K, and correspondingly, θ_a decreased from 40° to 18° and θ_r decreased from 33° to 12° (Figure 2).

On the coal surface, ionisable groups are present (e.g. phenolic and carboxylic groups, [27]), thus, as temperature increases and the pH decreases (pH decreases with temperature due to reduction in pK values of water and also due to a reduction in hydrogen bonding leading to increased number of protons (H^+); [28]), the released protons (H^+) interact with the surface functional groups and ionize them, e.g. C=O reacts to C-OH^+ or C-OH^+ reacts to C-OH_2^{2+} [27]. Therefore the surface of the coal becomes more positive with an increase in temperature, and consequently the zeta potential increases. Moreover, it is also reported that with increase in temperature, surface oxidation is accelerated and hydrophilic groups are formed on the coal surface at high temperature [29-31] which may lead to lower water contact angles with increasing temperature. However, we believe that oxidation of coal surfaces require sufficient exposure time which is likely to be well beyond the timescale of surface exposure to high temperature during our contact angle measurements [32]. Thus, we point out that oxidation may not be a governing factor for the decrease in contact angle with temperature despite a corresponding increase in zeta potential. We believe that further research is required to explore this effect.

Somasundaran et al. [31] found that for high volatile bituminous coal (from Pennsylvania), the magnitude of zeta potential decreased with temperature (at a pH of 6.78, zeta potential measured -26 mV at 300 K and reduced to -20 mV at 363 K). At the same pH (6.78, Table 2), the zeta potential of our medium rank coal (medium volatile bituminous) measured -24.8 mV at 298 K in good agreement with Somasundaran et al. [31]. The slight difference is probably due to the slightly different coal and associated differences in coal surface chemistry. Because of the limited literature data on zeta potential of coals, we compared our data with coals of similar ranks (if not exactly the same) despite their origin from a different basin (e.g. Somasundaran's coal from Pennsylvania is compared to our coal sample from West Virgina).

The observed increase in zeta potential with increasing temperature is attributed to the reduction in pH (with increasing temperature), consistent with Vinogradov and Jackson [33], who reported that zeta potentials of sandstones decreased in magnitude with increasing temperature for low salinity brine (0.6 wt% NaCl to 3 wt% NaCl), and they concluded that pH reduction with increasing temperature was responsible for the zeta potential variation. Note:

The coals are compared with quartz (Vinogradov and Jackson's [33] work) because mineralogy of these coals revealed that quartz is a significant component of these coals (XRD results, Table 3).

To further explain the charge reversal behaviour, we conducted pH measurements of the solutions at high temperatures and found that pH dropped only slightly (e.g. for lignite/water solution pH = 6.5 at 323 K and pH = 6.32 at 343 K), thus zeta potentials are only slightly impacted by pH changes. Therefore, divalent ions could possibly be acting as potential determining ions.

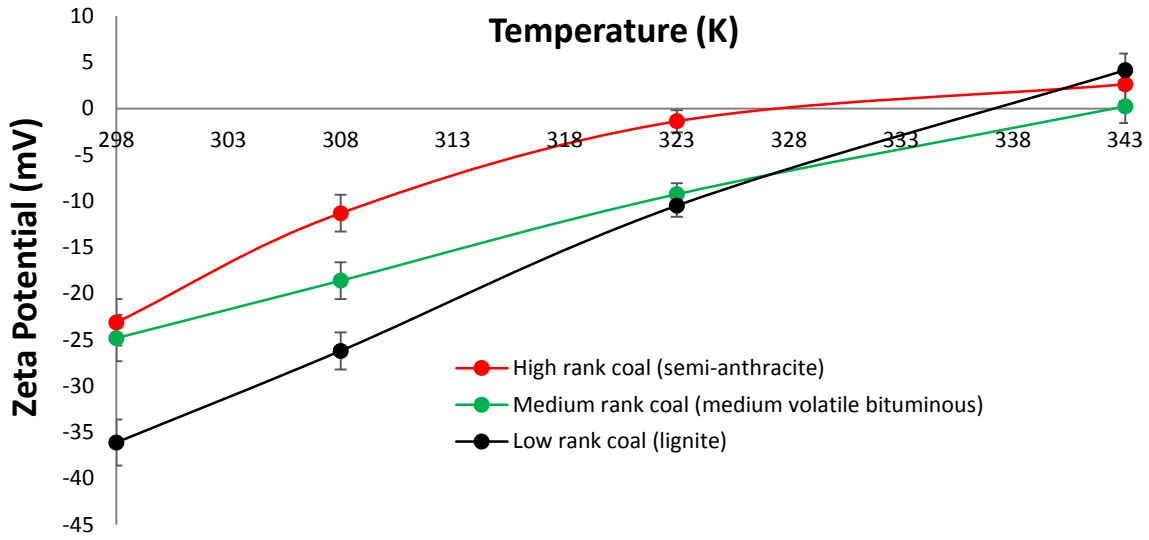

Figure 1. Zeta potential as a function of temperature and coal rank (at ambient pressure).

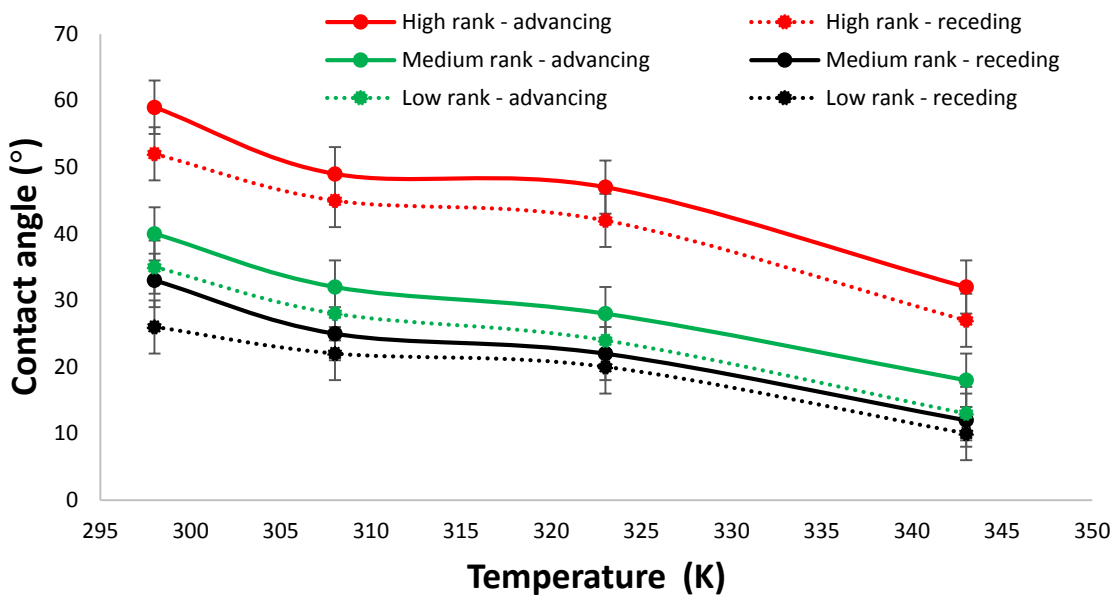

253

254 **Figure 2.** Water contact angle as a function of temperature and coal rank (at ambient pressure).

255

256 We further found that at any given temperature, high rank coal exhibited higher values of zeta
257 potential and higher water contact angles than low rank coals. For instance, at 323 K, the zeta
258 potential measured -1.36 mV for the high rank coal, -9.25 mV for medium rank coal, and 10.5
259 mV for low rank coal (Figure 1), while the associated contact angles were (θ_a = 47°, 28° and
260 24° and θ_r = 42°, 23° and 20° for high, medium and low rank coals respectively). This
261 behaviour is attributed to the lack of hydrophilic function groups (OH groups) in high rank
262 coals (further discussed in Section 3.5).

263 Considering the above electrochemical behaviour of coals at ambient pressure, we now
264 consider CO_2/brine/coal contact angle data at high pressure (15 MPa) from our previous work
265 (Arif et al., 2016c, [12]). It was found that at 15 MPa, for high rank coal, when temperature
266 increased from 308 K to 323 K, θ_a decreased from 146° to 119°, implying a wettability
267 transformation from strongly CO_2-wet to weakly CO_2-wet. Similarly, for medium rank coal, θ_a
268 decreased from 128° to 102° when temperature increased from 308 K to 343K. However, for
269 low rank coal, θ_a first decreased from 112° to 102° when temperature increased from 308 K to
270 323 K, and then became constant when temperature increased further (from 323 K to 343 K;
271 [12]). In summary, water-wettability of coal increased with increasing temperature irrespective
272 of the coal rank. Thus, the effect of temperature on wettability is similar at high pressure as
273 that found at ambient pressure (i.e. air/brine contact angles at low pressure and CO_2/brine

contact angles at high pressure followed similar trend). It can therefore be concluded that the temperature dependence of CO_2-wettability of coals is considerably controlled by electrochemical changes at the water/coal interface and that increase in temperature render the coal surface more water-wet due to formation of ionized surface functional groups.

3.2. Effect of salinity on zeta potential and contact angle

The effect of salinity on zeta potential and contact angle was studied as a function of brine salinity (0 wt% NaCl, 1 wt% NaCl and 5 wt% NaCl) at constant temperature (323 K). It was found that zeta potential increased with an increase in salinity for all coal ranks (Figure 3). Moreover, both θ_a and θ_r increased with salinity for all coal samples (Figure 4). Specifically, for the high rank coal, when salinity increased from 0 wt% NaCl to 5 wt% NaCl (or equivalently from 0M to 0.855M), zeta potential increased from -1.63 mV to 2.63 mV. For the same salinity increase, θ_a increased from 47° to 60° and θ_r increased from 42° to 53° (Figure 4). Similarly, for medium rank coal, the zeta potential increased from -9.25 mV to 0.263 mV when salinity increased from 0 wt% NaCl to 5 wt% NaCl, indicating a clear increase in zeta potentials with increasing salinity, and the corresponding values of θ_a increased from 28° to 41° and θ_r increased from 22° to 35° (Figure 4). Generally, for any solid/brine system, the composition of solid and the concentration and valency of ions in the solution are responsible for the sign and value of the zeta potential [34]. Physically, the coal surface exhibits negative charges due to the presence of polar functional entities, which partially dissociate, e.g. carboxylic or phenolic groups [35]; the concentration of these functional groups depends on the coal rank ([36] see also FTIR discussion in Section 3.5). The results found here are consistent with Ibrahim and Nasr-El-Din [37] who reported that both zeta potentials and contact angles on coals increased with salinity. Fuerstenau et al. [38] reported that for low ash anthracite coal, the zeta potential was measured to be -25 mV at 0.01 M NaCl (pH = 7) at room temperature. We found that for high rank coal (semi-anthracite) at (almost) the same pH (7.09, Table 2), the zeta potential was measured to be -23 mV (Figure 1) indicating consistent results. Harvey et al. [39] also found an increase in zeta potential of coal with salinity. They reported that for sub-bituminous (medium rank) coal, at a pH of 8, zeta potential increased from -32 mV to -25 mV when salinity changed from 0 wt% NaCl (DI-water) to 0.5 wt% NaCl at room temperature. For a similar bituminous coal we also measured an increase in zeta potential at 323K (-9.25 mV for DI-water decreased to -8.5 mV for 0.5 wt% NaCl brine, Figure 3). Roshan

et al. [40] recently introduced a model to describe the physical processes for wettability variation as a function of salinity and they related the contact angle to the electric potential at the mineral surface. According to their explanation, the dielectric constant of the fluid decreases with increasing salinity, which leads to an increased contact angle. The decrease in zeta potential correlates with the charge on the surface being more screened as more ions are present in the double layer, this leads to an increased water contact angle [41].

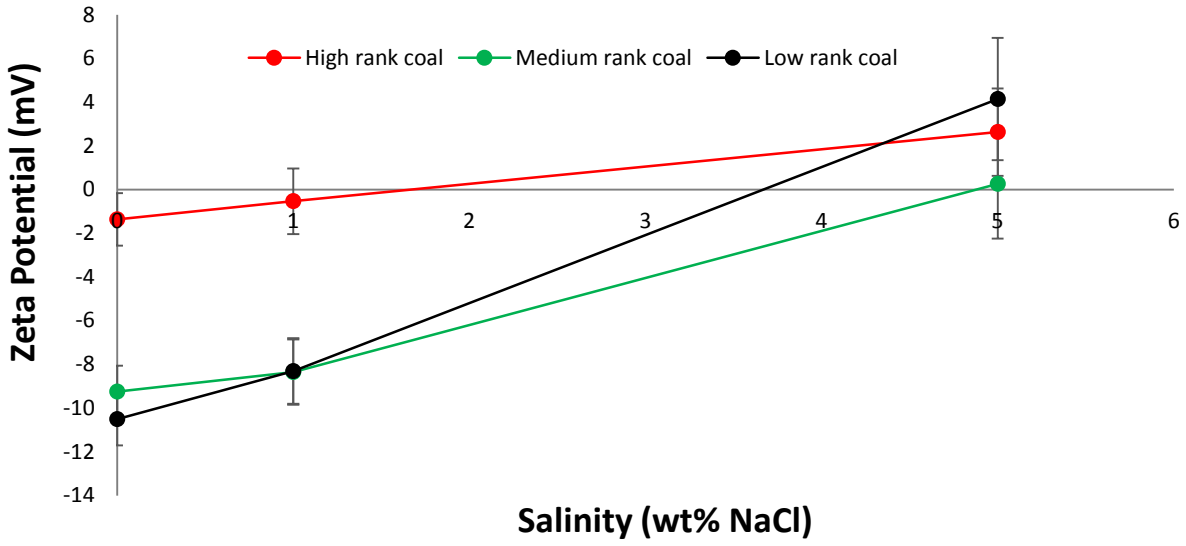

Figure 3. Effect of salinity on zeta potential at 323 K (and ambient pressure) as a function of coal rank.

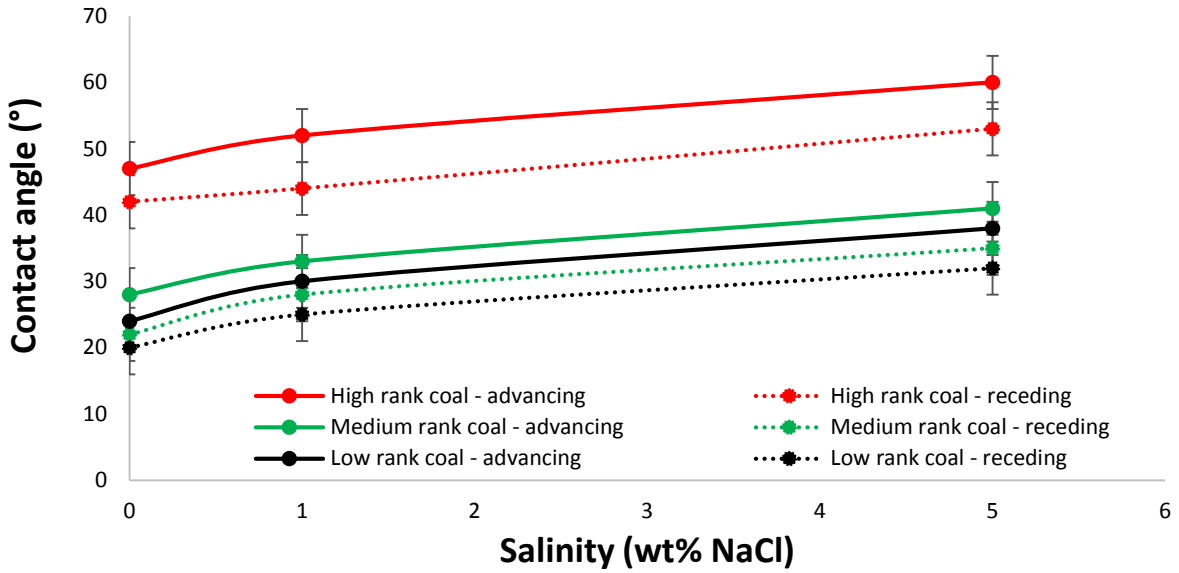

Figure 4. Water contact angle as a function of salinity and coal rank at 323 K (and ambient pressure).

Mechanistically, with the increase in ionic strength, the number of counter ions on the surface increases, which screens the surface charge (and thus results in a reduction of the thickness of the Debye layer). This means that the zeta potential decreases with increasing salt concentration. It is also notable that for the high rank coal, at a salinity of approximately 1.8 wt% NaCl the zeta potential is zero, while for low rank coal 3.7 wt% NaCl (Figure 3) is required to reach the point of zero zeta potential. The shift in salinity at which a zero charge is obtained varies between high, medium and low rank coal and is associated with the relative affinity of the respective coal surface for H^+ and OH^- ions (which varies with coal rank [23], and again is related to the concentration of surface functional groups, see FTIR discussion in Section 3.5). The salt content for achieving a zero charge as reported here is also of important consideration for processes that involve colloidal dispersion and coagulation [35], e.g. in coal processing [42].

Further, we compared zeta potentials to advancing and receding contact angles measured at high pressure (15 MPa and 323 K, Arif et al. [12]). For all coal ranks, both, θ_a and θ_r, increased with salinity at high pressures (Arif et al. [12]). For medium rank coal, at 15 MPa and 323 K, θ_a increased from 114° to 127° and θ_r increased from 102° to 112° when salinity increased from 0 wt% NaCl to 5 wt% NaCl brine. For a salinity increase from 5 wt% NaCl to 10 wt% NaCl, θ_a increased from 127° to 132° and θ_r increased from 112° to 116°. Moreover, we found similar

trends for low and high rank coals. Considering the fact that the trends of contact angle variation with temperature, salinity, and rank at high pressures were same as those at ambient conditions, it can be hypothesized that zeta potentials might also follow similar trends at high pressures (in a coal/CO_2/brine system) as we showed in this work at ambient pressure (in a coal/air/brine system).

3.3. Effect of brine composition on zeta potential and contact angle

The effect of salt type on zeta potential and contact angles was analysed by measuring zeta potentials and contact angles for coal/brine systems at 323 K and ambient pressure for three brines 1 wt% NaCl (0.17M), 1 wt% $CaCl_2$ (0.27M) and 1 wt% $MgCl_2$ (0.305M) for all coal ranks investigated. To facilitate the comparison of salt types, we have plotted zeta potential as a function of salt type in two formats: a) in terms of salt concentration in wt%, and b) in terms of the ionic strength of the solution (Figure 5 a, and b). We found that from Na to Ca to Mg brine types, at the same salinity and temperature, the zeta potential increased (Figure 5a) and contact angle also increased for all coal ranks (Figure 6). Specifically, for instance, for medium rank coal the zeta potential at the interface of coal/1 wt% NaCl-brine measured -8.3 mV, while at the coal/1 wt% $CaCl_2$-brine interface it measured -3.09 mV, and at coal/$MgCl_2$-brine interface it measured -2.65 mV indicating an increase in zeta potential with increasing cation charge-to-volume ratio (which is 2.61 x 10^{-7} C.pm^{-3} for Na^+, 4.92 x 10^{-7} C.pm^{-3} for Ca^+ and 1.66 x 10^{-6} C.pm^{-3} for Mg^+, [43]). At the ionic strength of 0.27M (1.58 wt%) NaCl, the zeta potential can be interpolated from Figure 3 (corresponding to 1.58 wt% NaCl) to facilitate comparison at exactly the same ionic strength as that of Ca and Mg based salts.

The negative values of the coal zeta potentials can be attributed to dissociation of surface functional groups (e.g. –COOH) [44]. The positive zeta potential values obtained are attributed to the surface charge screening effect due to counter ions provided by the cations of the salt as discussed above. Moreover, θ_a increased from 52° to 60° and θ_r increased from 44° to 53° when brine composition changed from 1 wt% NaCl to 1 wt% $MgCl_2$ (Figure 6). The results are consistent with [37] who also reported that coal/brine zeta potentials increased for divalent cations (Ca^{2+} and Mg^{2+}). Harvey et al. [39] also found that $MgCl_2$ brine resulted in an increase in zeta potential.

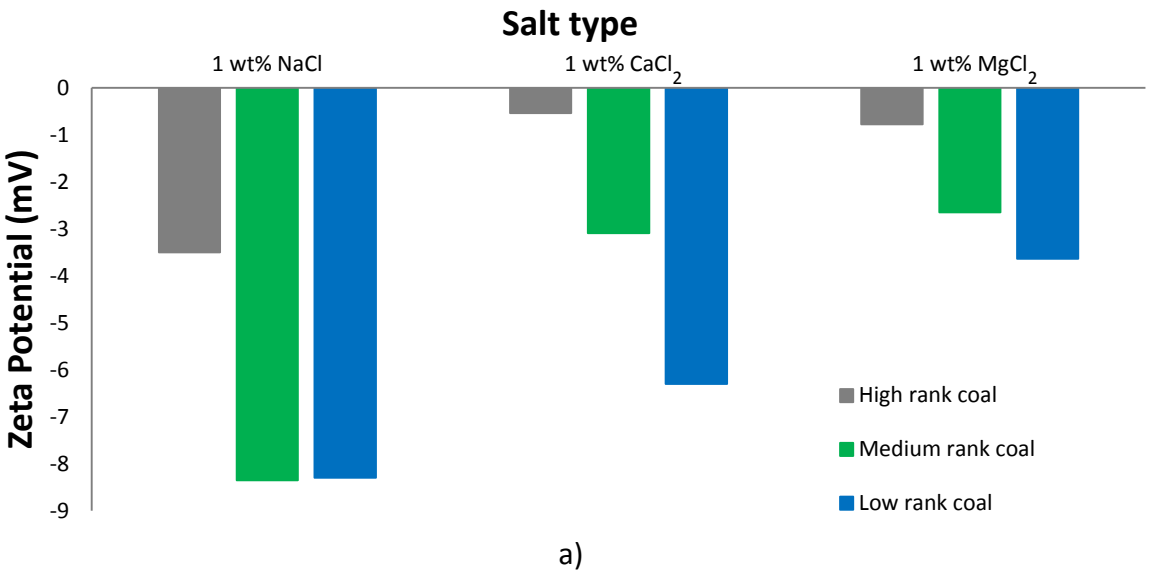

372

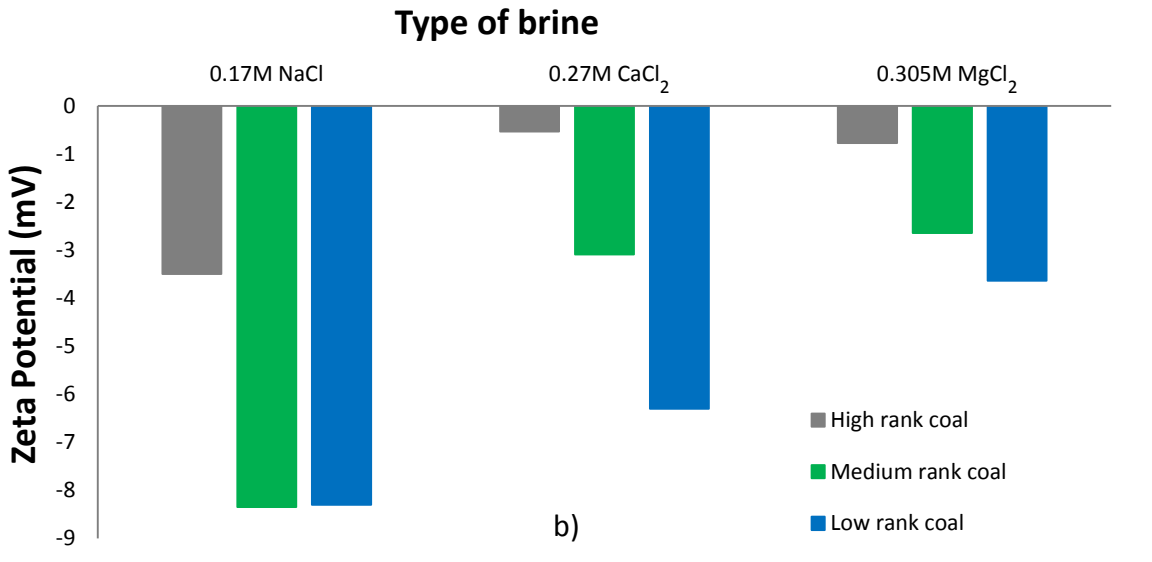

373

374 **Figure 5.** Zeta potential as a function of salt type (NaCl, $CaCl_2$, $MgCl_2$) and coal rank (at 323
375 K and ambient pressure). Data is shown in two formats: a) In terms of concentration in wt%,
376 b) In terms of ionic strength of brine

377

378

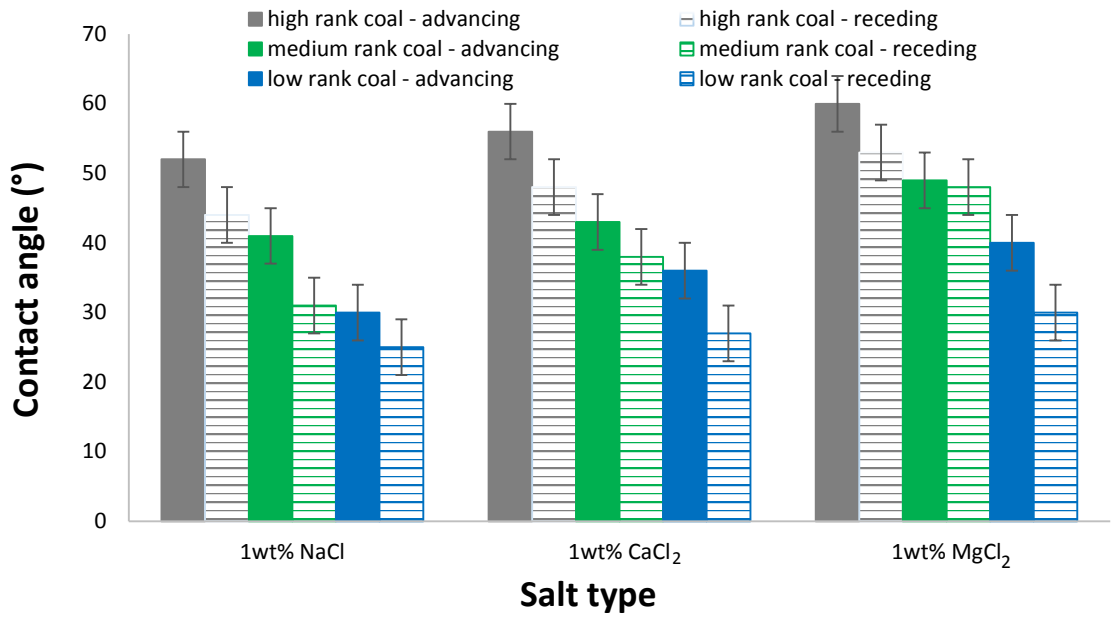

Figure 6. Water contact angle as a function of salt type (NaCl, $CaCl_2$, $MgCl_2$) and coal rank (at 323 K and ambient pressure).

3.4 Zeta potential and contact angles as a function of coal rank

To investigate the impact of coal rank on zeta potential and wettability, the results shown in Figures 1-6 are reconsidered briefly. At any temperature (except 343 K), the zeta potential of the coal/water system increased with increasing rank (Figure 1). For instance, at 308 K, the zeta potential was -26.2 mV for low rank coal (lignite, R_o = 0.35%), -18.6 mV for medium rank coal (medium volatile bituminous, R_o = 0.82%) and -11.3 mV for high rank coal (semi-anthracite, R_o = 3.92%). This is consistent with Abotsi et al. [45] who found that at a pH > 5.5 low rank coal had more negative zeta potential values in DI water at room temperature. For instance, they reported that at a pH = 6.5, zeta potentials of lignite (North Dakota) were -40 mV, ~ -30 mV for sub-bituminous and ~ -20 mV for bituminous coals which is quite comparable to our results (at 298 K, zeta potentials measured -36 mV and -25 mV for low and medium rank coals, respectively).

As the coal rank increases, the zeta potential increases, indicating a diminishing number of polar surface sites (a proportion of which are negatively charged due to dissociation), [42]. This results in a strong dependence of the isoelectric point (the pH at which the surface carries no net charge) and the sign of the zeta potential on the carbon content (i.e. the coal rank, [46]).

In addition, aqueous cationic ion concentrations increase due to dissociation of groups capable of forming ions or decrease by re-adsorption of some dissolved ions on the solid particle surface [47]. Consequently the electrical double layer on the particle becomes thinner or thicker, which induces a change in zeta potential. In the case of coal, the high mineral content and dissociation of ionogenic groups on the (complex) coal surface [48] leads to different charges on coals of different ranks (low zeta potentials for low rank coal and high zeta potentials for high rank coal).

We relate the variation in zeta potential as a function of coal rank to the mineralogy of coal. In this context, we note that the major components of the coals are quartz and kaolinite (XRD results, Table 3). The low rank coal contains 76% quartz and 24% kaolinite. At room temperature, we find from Kaya and Yukselen [49] that zeta potential of quartz/water and kaolinite/water were both negative for a wide range of tested pH and that quartz/water zeta potential was much lower than that of the kaolinite/water (e.g. at pH of 6.8, zeta potentials were -52 mV for quartz and -34 mV for kaolinite). Thus our measured value of zeta potential of lignite which was -36.1 mV at room temperature is in accordance to the mineralogy of lignite i.e. the zeta potential of lignite is comparable to individual mineral's zeta potentials. Moreover the percentages of quartz and kaolinite were 41 wt% and 30 wt% in medium rank coals, and 21 wt% and 24 wt% in high rank coals (Table 3). The measured values of zeta potential of medium and high rank coal at 298 K were -24.8 mV and -23.1 mV. The impact of minerology is thus clear in the sense that the increase in percentage of quartz and kaolinite in coal leads to a reduction in zeta potential (low rank coal has lower zeta potential because of higher quartz and kaolinite content).

The decrease in negative charge density on the coal surface with increasing coal rank is attributed to the increase in fixed carbon (%) and a decrease in oxygen content with rank [50], Table 1. We note that high and medium rank coal demonstrated similar trend of zeta potential variation as a function of salinity but low rank coal showed slightly inconsistent behaviour as a function of salinity at higher salinity (5wt% NaCl) which can be attributed to the presence of more hydrophilic groups (OH groups) in low rank coals, Figure 3).

The surface charge on coal in the presence of electrolytes is induced by ionization or protonation of the surface carboxylic and hydroxyl groups; note that the dissociation of carboxylic groups is enhanced in the presence of OH^- [51].

$$-COOH_2^+ \overset{H^+}{\leftarrow} -COOH \overset{OH^-}{\longrightarrow} -COO^- + H_2O$$

$$-COH_2^+ \overset{H^+}{\leftarrow} -COH \overset{OH^-}{\longrightarrow} -CO^- + H_2O$$

3.5. Surface functional group characterization and associated hydrophobicity of coals

In order to assess the factors responsible for the wetting behaviour of the coal/CO_2/brine systems, we consider experimental data for water advancing and receding contact angle from our previous work (Arif et al. [12]), Figure 7. It can be seen that water wettability of coals decreases with increasing pressure and increasing rank. At any given CO_2 pressure, the high rank coal had the highest water contact angle which means that these coals are less water-wet. Low rank coals (e.g. lignite) are more water-wet and medium rank coal (e.g. bituminous) are intermediate-wet. These results are in agreement with Shojai Kaveh et al. [15] who compared CO_2-wettability of semi-anthracite and high volatile bituminous coals, and they measured higher contact angles for semi-anthracite coals, and thus they concluded that hydrophobicity of coals increases with coal rank. However, the surface functional groups responsible for such wetting behaviour were unclear. We thus conducted FTIR (Fourier transformed infrared) spectroscopy measurements on the three coal samples, the results are presented in Figure 8.

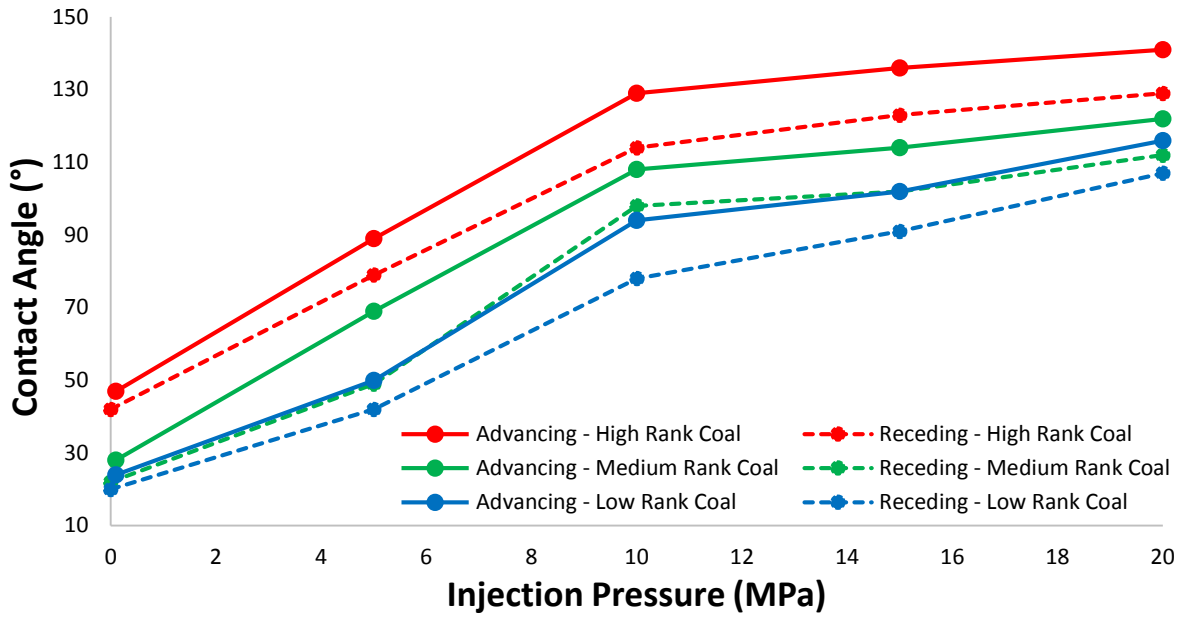

Figure 7. Water contact angle as a function of pressure and coal rank at 323 K (experimental data from Arif et al. [12]).

High rank coal (semi-anthracite) demonstrated a rather smooth FTIR intensity response throughout the observed wavenumber spectrum, with only small bands observed at a wavenumber range of at 600-800 cm^{-1} due to a possible C-S stretching vibration, the 1000-1100 cm^{-1} due to C-H out of plane bending and Si-O-H asymmetric stretch vibrations and a minute band at ~ 3800 cm^{-1} due to –OH and N-H bond stretching vibrations [52,53]; considering the fact that XRD confirmed the presence of Si (Table 3) and elemental analysis confirmed the presence of sulphur and nitrogen (Table 1). The rough part of the spectra for 2000-2400 cm^{-1} should be ignored as this is where the ATR crystal is absorbing itself (diamond) and the bands don't always perfectly cancel out. From the stand point of surface functional groups and associated wetting behaviour, the absence (or only minute presence) of hydrophilic sites e.g. OH groups in high rank coal is responsible for its hydrophobic behaviour (θ>130°, Figure 7).

On the contrary, medium rank coal (medium volatile bituminous) exhibited significantly stronger bands (in comparison to high rank coal) at wave numbers from 600-800 cm^{-1} and 1000-1100 cm^{-1} indicating the presence of more C-S stretching vibrations and C-H out of plane bending. Moreover, medium rank coal also exhibited larger bands at ~3600-3700 cm^{-1} which is attributed to O-H and N-H stretch vibrations. Furthermore, distinct bands were observed at 2800-2900, and 1500-1700 cm^{-1} which are due to C=C and C=O stretch vibrations respectively [53]. Thus, the presence of more hydrophilic sites (OH groups) in medium rank coal renders it relatively less CO_2-wet in comparison to high rank coal (e.g. for instance at 10 MPa, θ_a = 108° for medium rank coal in comparison to 129° for high rank coal, Figure 7).

Low rank coal demonstrated the largest peak beginning at about 2800 cm^{-1} and ending at 3800 cm^{-1} which is attributed to the O-H and N-H stretch vibrations and this largest peak is responsible for the hydrophilic nature of lignite coal even at high pressures (Figure 7). The band at ~2900 cm^{-1} observed for low rank coal is due to the presence of aliphatic C-H stretching vibrations [36]; however, its absence in high rank coal is unusual and is perhaps due to C-H stretching where the carbon is in a C=C bond. Moreover, the sharp band observed at 1500-1800 cm^{-1} for low rank coal is attributed to aromatic ring vibrations, which are enhanced by oxygen groups [35]. The corresponding shoulder peaks at 1600 cm^{-1} is attributed to C=O stretching vibrations and these represent all C=O functionalities, e.g. carboxylic acids or phenolic esters [54,55]. Chemically, the presence of such polar functional groups leads to an

increase in hydrophilicity of the coals' surface and that is evident from the contact angle data (e.g. lignite is relatively more water-wet as compared to bituminous and anthracite coals, Figure 7).

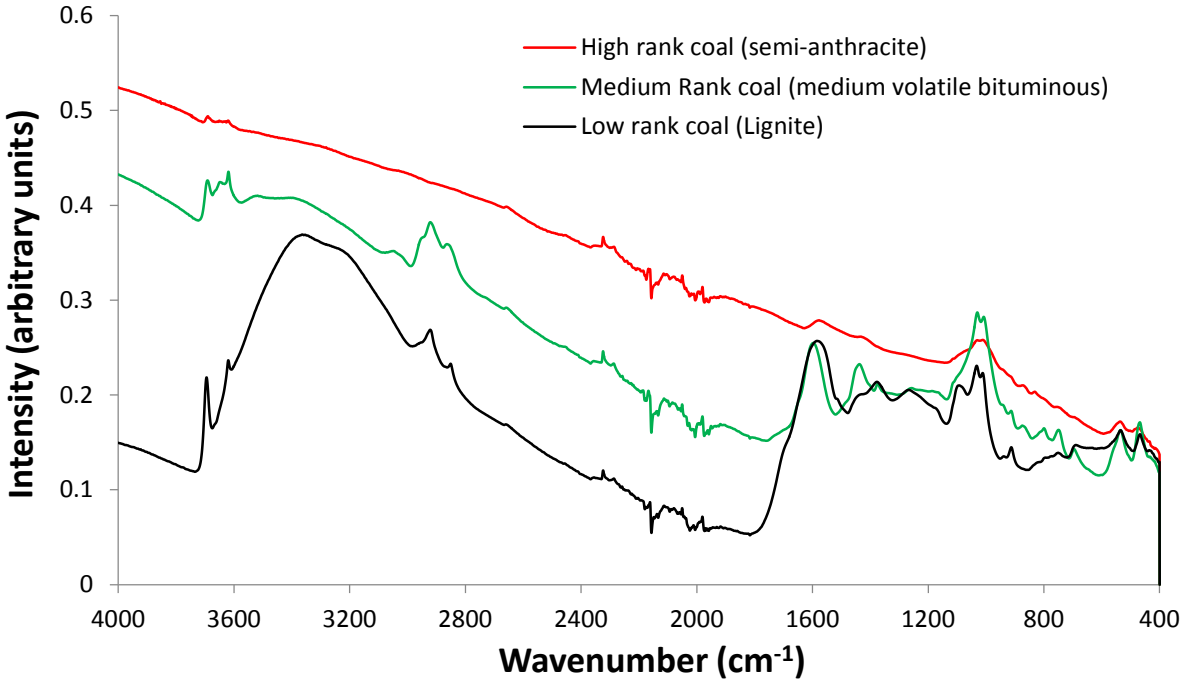

Figure 8. ATR-infrared spectroscopy measurements on low, medium and high rank coals

In summary, the much lower number of Si-OH, hydroxyl, ester, and carboxylic groups in high rank coal is responsible for its hydrophobic behaviour. On the contrary, the abundance of these groups (especially OH) is responsible for the hydrophilic nature of low rank coal. Medium rank coal stands somewhere in the middle (consistent with contact angle data; Figure 8). Thus the increase in contact angle (at typical operating conditions) with coal rank (Figure 7, Arif et al. [12]) is adequately explained by surface functional groups.

3.6 Correlation between zeta potential and coal-wettability

Our results showed that zeta potential increased with increasing rank and salinity, and contact angle also increased with increasing rank and salinity, implying a positive correlation between zeta potential and coal-wettability, i.e. higher zeta potential correspond to a less water-wet surface (= higher θ). In order to demonstrate this relation, we developed a cross plot between

499 water advancing contact angle and zeta potential as a function of rank (Figure 9a) and as a
500 function of salinity (Figure 9b).

501 Specifically, for any given temperature (298 K-343 K), advancing contact angle increased with
502 the increase in zeta potential (all solid coloured trend lines in Figure 9a) for all coals. Moreover,
503 as salinity increased, zeta potential increased and contact angle also increased (Figure 9b). The
504 overall correlation between zeta potential and wettability is also positive (Figure 9b).

505 However, with respect to temperature, a contradictory trend is found such that as temperature
506 increased zeta potential increased but contact angle decreased (this can be visualized by joining
507 the points of the same symbol in Figure 9a by means of a trend line). The reason for this
508 contradiction is not clearly known yet, however, the possible factors responsible for this
509 deviation could be evaporation at high temperature, and/or the experimental error associated
510 with equipment at high temperatures (which we found was relatively high).

511 On a whole, it appears as if zeta potential is not the primary driver of coal-wettability despite
512 clear positive correlation with respect to salinity and coal rank. Thus it can be established that
513 zeta potential is a secondary factor which controls the coal-wettability variation to some extent.
514 The primary control of wettability is governed by the interfacial interactions of fluids with
515 surface [56] as a function of pressure, temperature and salinity.

516

517

518

519

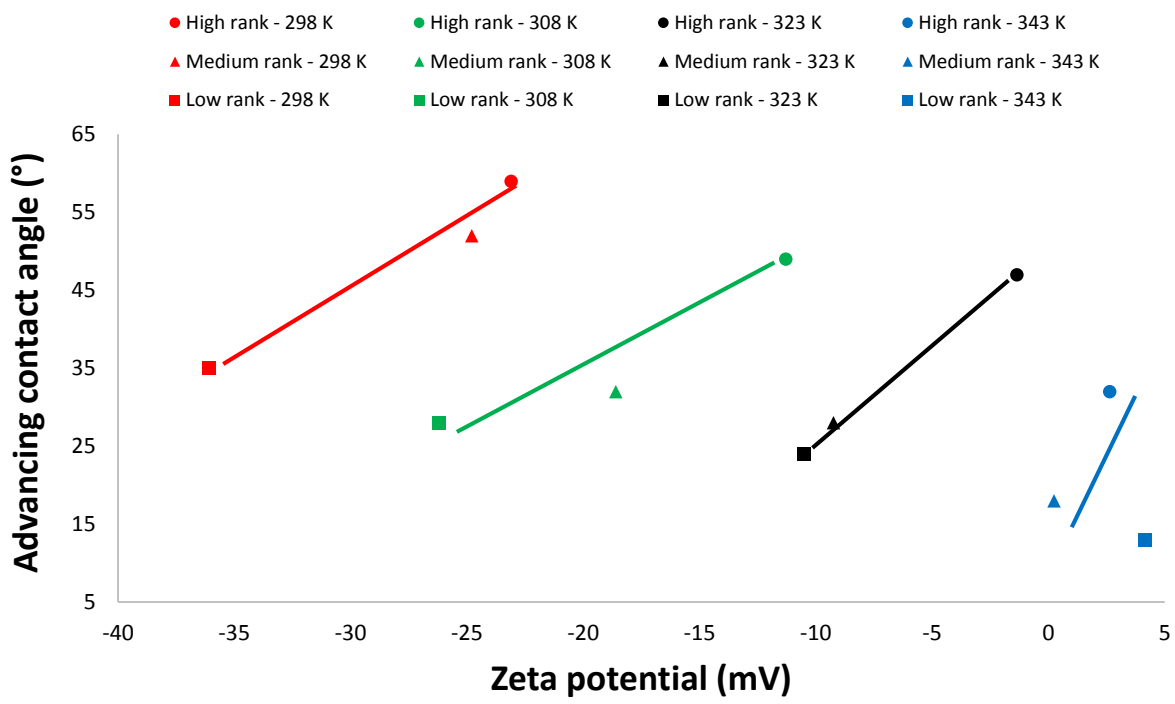

520

521 **Figure 9a.** Contact angle-zeta potential cross plot at all temperatures as a function of coal rank.
522 Circle = high rank, triangle = medium rank, square = low rank coal. The colour differentiates
523 the measurements as a function of temperature (red, green, black and blue). The solid lines are
524 the trend lines for relation between zeta potential and wettability as a function of coal rank at
525 isothermal and iso-saline conditions.

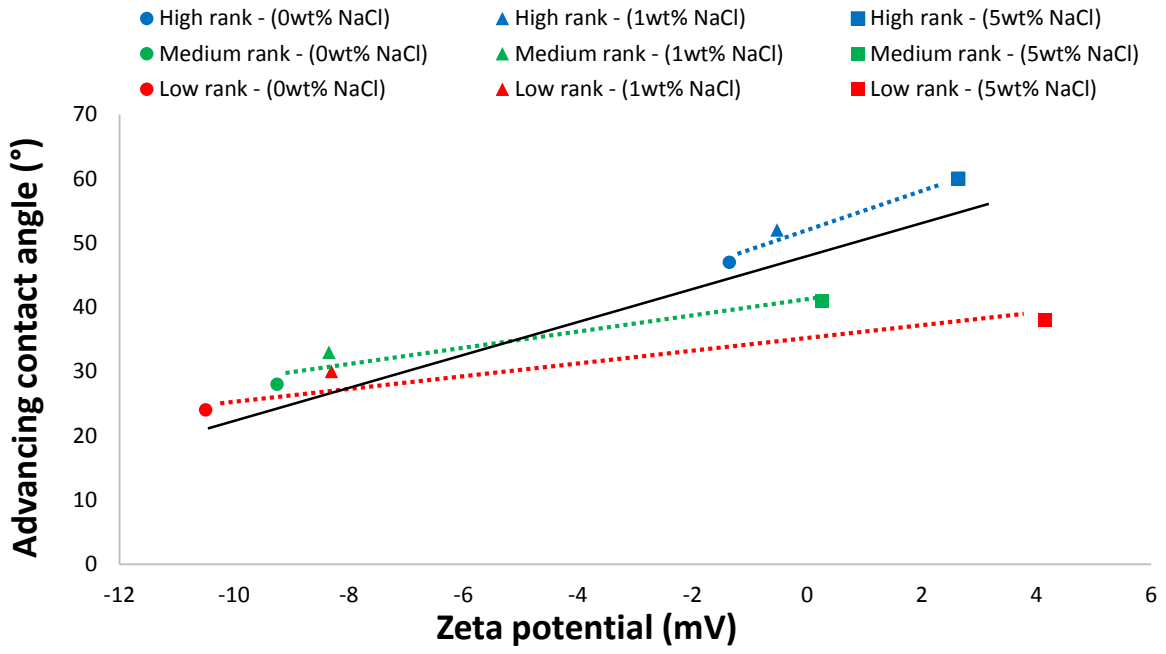

526

527 **Figure 9b.** Contact angle-zeta potential cross plot as a function of salinity for all coal ranks at
528 323 K. The symbol differentiates the measurements as a function of salinity (Circle: DI-water,

triangle: 1wt% NaCl, square: 5wt% NaCl). The dotted lines are the trend lines for relation between zeta potential and wettability as a function of salinity for all ranks at isothermal conditions. The solid black line represent the overall trend.

4. Implications

In order to assess the factors affecting wetting behaviour of coals, which is of immense importance in terms of understanding micro- and nano-scale fluid dynamics in coal seams, we provided insight into the fluid interactions at the coal/brine interface and their relation with wetting behaviour as a function of temperature, salinity and coal rank. The measured data essentially leads to a better understanding of the mechanism occurring at the pore scale and is, therefore, useful for understanding CO_2 storage and (enhanced) methane recovery in coal beds. Zeta potential measurements provide a better understanding of the effect of salinity and rank on wettability, however trend of zeta potential with temperature when correlated with contact angle data was contradictory which needs further investigation. Moreover, the presence of typical surface functional groups (e.g. OH and carboxylic groups) is responsible for the specific wettability of coals (Figure 7), and this data can thus be used to assess the storage potential of coal seams.

Specifically, we observed that high rank coal was CO_2-wet (at reservoir conditions), and thus once injected, CO_2 occupies the smallest pores (nano- and micropores in the coal seams) due to its larger affinity to adsorb onto the coal surface [57,58]. As a result, methane is displaced towards the production wells and thus leads to improved methane production. However, the lower coal ranks are relatively less suitable for enhanced methane recovery and CO_2-storage due to their more water-wet characteristics, which implies poorer adsorption of CO_2 onto the coal micro surface [59]. We also point out that with the increase in pressure coal swelling occurs which leads to a reduction in permeability; and this effect limits CO_2 injection into coal seams [60].

5. Conclusions

We measured zeta potentials as a function of temperature and salinity for low, medium and high rank coals. It was found that zeta potential increased with temperature and the water contact angle decreased with temperature. Zeta potentials increased with increasing salinity due to reduction in the thickness of the Debye layer, which occurred because of the surface charge screening by the counter ions. The coal/brine/CO_2 water contact angle also increased with increasing salinity. Furthermore Mg^{2+} brine demonstrated higher contact angles and higher zeta potentials than those of Ca^{2+} and Na^{+} brines, and, at any temperature or salinity, high rank coals exhibited high zeta potentials, which is due to their higher carbon content and associated lower surface charge (due to absence of polar functional groups). Zeta potential increased with salinity and rank, and contact angles also increased with salinity and rank, implying a positive relation between zeta potential and wettability. However, the effect of temperature was not conclusive in that the zeta potential increased with temperature but the contact angles decreased with temperature. Thus, despite zeta potential appears to have significant relation with contact angles, yet, it may not be considered as a primary driver of wettability and that further investigation is required to explore this effect.

The contact angle trends with temperature and salinity at ambient conditions were similar to those at high pressures and thus we hypothesized that zeta potential measurements at ambient conditions should follow similar trends at high pressure conditions. Furthermore, we conducted ATR-FTIR spectroscopy measurements on the coal substrates, and we measured an abundance of OH groups on the low rank coal, which is responsible for their hydrophilic nature, while high rank coals exhibited minimal OH peaks (and thus absence of OH groups), which explains their hydrophobic nature.

We furthermore provided implications of the measured data for CO_2-storage and enhanced methane recovery and it can be concluded that high rank coal seams (at low temperature and high pressure) are most feasible for CO_2-storage and enhanced methane recovery due to better CO_2-wettability and thus improved CO_2-adsoprtion capacity.

References

1) Blunt MJ, Fayers FJ, Orr FM. Carbon dioxide in enhanced oil recovery. Energy Convers Manage 1993;34:1197-1204.

2) Iglauer S, Paluszny A, Blunt MJ. . Simultaneous oil recovery and residual gas storage: A pore-level analysis using in situ X-ray micro-tomography. Fuel 2013;103:905-914.

3) Metz B, Davidson O, de Coninck H, Loos M, Meyer L. Intergovernmental panel on climate change special report on carbon dioxide capture and storage. Cambridge University Press; 2005.

4) Arif M, Al-Yaseri AZ., Barifcani A, Lebedev M, Iglauer S. Impact of pressure and temperature on CO_2–brine–mica contact angles and CO_2–brine interfacial tension: Implications for carbon geo-sequestration. J Colloid Interface Sci 2016a;462:208-215.

5) Arif M, Barifcani A, Lebedev M, Iglauer S. Structural trapping capacity of oil-wet caprock as a function of pressure, temperature and salinity. Int J Greenh Gas Con 2016b;50:112-120.

6) Hesse MA, Orr FM, Tchelepi HA. Gravity currents with residual trapping. J Fluid Mech 2008;611:35-60.

7) Iglauer S, Al-Yaseri AZ, Rezaee R, Lebedev M. CO_2 wettability of caprocks: Implications for structural storage capacity and containment security. Geophys Res Lett 2015b;42:9279-9284.

8) Iglauer S, Paluszny A, Pentland CH, Blunt MJ. Residual CO2 imaged with X-ray micro-tomography. Geophys Res Lett 2011a;38:21.

9) Iglauer S, Wülling W, Pentland CH, Al-Mansoori SK, Blunt MJ. Capillary-trapping capacity of sandstones and sandpacks. SPE J 2011b;16:778-783.

10) Iglauer S. Dissolution trapping of carbon dioxide in reservoir formation brine-a carbon storage mechanism. In: Nakajima H, editor. Mass transfer – advanced aspects. Rijeka: InTech; 2011c.

11) Gaus I. Role and impact of CO_2–rock interactions during CO_2 storage in sedimentary rocks. Int J Greenh Gas Con 2010;4:73-89.

12) Arif M, Barifcani A, Lebedev M, Iglauer S. CO_2-wettability of low to high rank coal seams: Implications for carbon sequestration and enhanced methane recovery. Fuel 2016c;181:680-689.

13) Saghafi A, Javanmard H, Pinetown K. Study of coal gas wettability for CO_2 storage and CH_4 recovery. Geofluids 2014;14:310-325.

14) Shojai Kaveh N, Rudolph ESJ, Wolf KHA, Ashrafizadeh SN. Wettability determination by contact angle measurements: hvBb coal–water system with injection of synthetic flue gas and CO_2. J Colloid Interface Sci 2011;364:237-247.

15) Shojai Kaveh N, Wolf KH, Ashrafizadeh SN, Rudolph ESJ. Effect of coal petrology and pressure on wetting properties of wet coal for CO2 and flue gas storage. Int J Greenh Gas Con 2012;11:S91-S101.

16) Adamson AW, Gast, AP. The solid–liquid interface-contact angle. Phys Chem Surf 1997;4:333-361.

17) Iglauer S, Pentland CH, Busch A. CO_2 wettability of seal and reservoir rocks and the implications for carbon geo-sequestration. Water Resour Res 2015a;51:729-774.

18) Erbil HY. Solid and liquid interfaces. Oxford: Blackwell; 2006.

19) Alkan M, Demirbaş Ö, Doğan M. Electrokinetic properties of kaolinite in mono-and multivalent electrolyte solutions. Micropo Mesopor Mat 2005;83:51-59.

20) Buckley JS, Liu Y, Monsterleet S. Mechanisms of wetting alteration by crude oils. SPE J 1998;3:54-61.

21) Nasralla RA, Nasr-El-Din HA. Double-layer expansion: is it a primary mechanism of improved oil recovery by low-salinity waterflooding?. SPE Reserv Eval Eng 2014;17:49-59.

22) Bustin RM, Barnes MA, Barnes WC. Diagenesis 10. Quantification and modelling of organic diagenesis. Geoscience Canada 1985;12.

23) Lander LM, Siewierski LM, Brittain WJ, Vogler EA. A systematic comparison of contact angle methods. Langmuir 1993;9:2237-2239.

24) Iglauer S, Salamah A, Sarmadivaleh M, Liu K, Phan C. Contamination of silica surfaces: Impact on water–CO_2–quartz and glass contact angle measurements. Int J Greenh Gas Con 2014;22:325-328.

25) Drelich J, Laskowski JS, Pawlik M, Veeramasuneni S. Preparation of a coal surface for contact angle measurements. J Adhes Sci Technol 1997;11:1399-1431.

26) Rodríguez K, Araujo M. Temperature and pressure effects on zeta potential values of reservoir minerals. J Colloid Interface Sci, 2006;300:788-794.

27) Laskowski J. Coal flotation and fine coal utilization. Vol. 14. Gulf Professional Publishing, 2001.

28) Akiya N, Savage PE. Roles of Water for Chemical Reactions in High-Temperature Water. Chem Rev 2002;102:2725-2750.

29) Ding LP. Investigation of bituminous coal hydrophobicity and its influence on flotation. Energy Fuels 2009;23:5536-5543.

30) Ramesh R, Somasundaran P. Chemical and wettability studies on coal, humic acid and cyclized humic acid. Fuel 1989;68:533-535.

31) Somasundaran P, Roberts CE, Ramesh R. Effects of oxidizing methods on the flotation of coal. Miner Eng 1991;4:43-48.

32) Calemma V, Rausa R, Margarit R, Girardi E. FT-ir study of coal oxidation at low temperature. Fuel 1988;67:764-770.

33) Vinogradov J, Jackson MD. Zeta potential in intact natural sandstones at elevated temperatures. Geophys Res Lett 2015;42:6287-6294.

34) Butt HJ, Graf K, Kappl M. Physics and chemistry of interfaces. John Wiley & Sons 2006.

35) Sarwar, A., Khan, M. N., & Azhar, K. F. (2012). Coal chemistry and morphology of thar reserves, Pakistan. Journal of Minerals and Materials Characterization and Engineering, 11(08), 817.

36) Wu D, Liu G, Sun R. Investigation on structural and thermodynamic characteristics of perhydrous bituminous coal by Fourier transform infrared spectroscopy and thermogravimetry/mass spectrometry. Energy Fuels 2014;28:3024-3035.

37) Ibrahim AF, Nasr-El-Din HA. Effects of Water Salinity, CO_2 Solubility, and Gas Composition on Coal Wettability. In EUROPEC 2015. SPE 2015.

38) Fuerstenau DW, Rosenbaum JM, Laskowski J. Effect of surface functional groups on the flotation of coal. Colloid Surface, 1983;8:153-173.

39) Harvey PA, Nguyen AV, Evans GM. Influence of electrical double-layer interaction on coal flotation. J Colloid Interface Sci 2002;250:337-343.

40) Roshan H, Al-Yaseri AZ, Sarmadivaleh M, Iglauer S. On wettability of shale rocks. J Colloid Interface Sci 2016;475:104-111.

41) Mugele F, Baret JC, (2005). Electrowetting: from basics to applications. Journal of Physics: Condensed Matter, 17(28), R705.

42) Chi SM, Morsi BI, Klinzing GE, Chiang SH. Study of interfacial properties in the liquid carbon dioxide-water-coal system. Energy Fuels 1988;2:141-145.

43) Al-Yaseri AZ, Lebedev M, Barifcani A, Iglauer S. Receding and advancing (CO_2+ brine+ quartz) contact angles as a function of pressure, temperature, surface roughness, salt type and salinity. J Chem Thermodyn 2016;93:416-423.

44) Crawford RJ, Mainwaring DE. The influence of surfactant adsorption on the surface characterisation of Australian coals. Fuel 2001;80:313-320.

45) Abotsi GM, Bota KB, Saha G. Interfacial phenomena in coal impregnation with catalysts. Energy Fuels 1992;6:779-782.

46) Crawford RJ, Guy DW, Mainwaring DE. The influence of coal rank and mineral matter content on contact angle hysteresis. Fuel 1994;73:742-746.

47) Xu R, Hu B, He Q, Cai J, Pan Y, Shen J. Effect of compound inorganic nano-stabilizer on the stability of high concentration coal water mixtures. Fuel 2006;85:2524-2529.

48) Doymus K. The effect of ionic electrolytes and pH on the zeta potential of fine coal particles. Turk J Chem 2007;31:589-597.

49) Kaya, A., & Yukselen, Y. (2005). Zeta potential of clay minerals and quartz contaminated by heavy metals. Can Geotech J, 42(5), 1280-1289.

50) Fuerstenau DW, Rosenbaum JM, You YS. Electrokinetic behavior of coal. Energy Fuels 1988;2:241-245.

51) Puri BR. Surface complexes on carbons. Chem Phys Carbon 1970;6:191-282.

52) Griffiths PR, De Haseth JA. Fourier transform infrared spectrometry. John Wiley & Sons 2007;171.

53) Socrates G. Infrared and Raman characteristic group frequencies: tables and charts. John Wiley & Sons. 2004.

54) Manoj B, Kunjomana AG, Chandrasekharan KA. Chemical leaching of low rank coal and its characterization using SEM/EDAX and FTIR. J Min Mat Charact Eng 2009;8:821.

55) Tsai SC. Fundamentals of coal beneficiation and utilization. Elsevier Science & Technology 1982;2.

56) Arif M, Barifcani A, Iglauer S. Solid/CO2 and solid/water interfacial tensions as a function of pressure, temperature, salinity and mineral type: Implications for CO2-wettability and CO2 geo-storage, Int J Greenh Gas Con 2016;53:263.

57) Busch A, Gensterblum Y, Krooss BM. Methane and CO_2 sorption and desorption measurements on dry Argonne premium coals: pure components and mixtures. Int J Coal Geol 2003;55:205-224.

58) Clarkson CR, Bustin RM. Binary gas adsorption/desorption isotherms: effect of moisture and coal composition upon carbon dioxide selectivity over methane. Int J Coal Geol 2000;42:241-271.

59) Mastalerz M, Gluskoter H, Rupp J. Carbon dioxide and methane sorption in high volatile bituminous coals from Indiana, USA. Int J Coal Geol 2004;60:43-55.

60) Reucroft PJ, Sethuraman AR. Effect of pressure on carbon dioxide induced coal swelling. Energy Fuels 1987;1:72–5.